INSOLATION AND RESULTING SURFACE TEMPERATURES OF STUDY REGIONS ON MERCURY.

K. E. Bauch[1], H. Hiesinger[1], and J. Helbert[2]. [1]Institut für Planetologie, Westfälische Wilhelms-Universität, Wilhelm-Klemm-Str. 10, 48149 Münster, Germany. [2]DLR-Institut für Planetenforschung, Rutherfordstr. 2, 12489 Berlin, Germany. karin.bauch@uni-muenster.de

Introduction: The imaging spectrometer MERTIS (Mercury Radiometer and Thermal Infrared Spectrometer) is part of the payload of ESA's BepiColombo mission, which is scheduled for launch in 2014 [1]. The instrument consists of an IR-spectrometer and radiometer, which observe the surface in the wavelength range of 7-14 and 7-40µm, respectively. The four scientific objectives [1, 2] are to

a) study Mercury's surface composition,

b) identify rock-forming minerals,

c) globally map the surface mineralogy and

d) study surface temperature and thermal inertia.

In preparation of the MERTIS experiment, we performed detailed thermal models of the lunar surface, which we extrapolated to Mercury. For our simulation, we use topography data from the Moon and idealized crater geometries and transfer them as model regions to the surface of Mercury. When calculated with lunar parameters, this allows us to compare the results to lunar temperature measurements of the Apollo, Clementine and Chandrayaan missions [e.g., 3-5]. It also allows a direct comparison of the insolation and thermal variation between craters on the lunar and Mercurian surface.

Background: Previous studies of the lunar surface have shown that thermal emission contributes to the observed signal from the surface and can influence the spectral characteristics, e.g., the depth of absorption bands [e.g., 5-7]. Therefore accurate knowledge of the solar insolation and resulting thermal variations is necessary for the correct interpretation of long-wavelength spectral data. In order to calculate insolation and surface temperatures, we use a numerical model which has been described by [8]. Surface temperatures are dependent on the surface and subsurface bulk thermophysical properties, such as bulk density, heat capacity, thermal conductivity, emissivity, and albedo. Topography also influences surface temperatures, as it changes the angle of solar incidence, but also leads to shadowed areas, e.g., the floors of polar craters.

Method: In order to determine surface and subsurface temperatures, the model solves the one-dimensional heat transfer equation. It includes the bulk density ρ, heat capacity C, and thermal conductivity k, which are dependent on depth and/or temperature. The thermophysical parameters can be summarized to a thermal inertia representing the ability of the surface to adapt to temperature changes. Thermal inertia I is an important property for determining temperature variations of planetary surfaces and is defined as

$$I \equiv \sqrt{k\rho C} \qquad (1)$$

The surface boundary condition is based on the energy balance relation; the energy entering the surface equals the energy leaving the surface:

$$\frac{S_0}{R^2}\cos(i)\,(1-A) + k\frac{\partial T}{\partial z} = \varepsilon\sigma T_0^4 \qquad (2)$$

The first term is an insolation function, which includes the solar flux S_0 at 1 AU, and the surface albedo A. The orbital radius R and solar inclination i are calculated from JPL's Horizons software and updated in each time step. The second term represents subsurface conduction and the last term radiation loss into space, including the soil's emissivity ε and Stefan-Boltzmann constant σ. The bottom layer boundary condition is given by a constant planetary heat flow from below.

In addition to the direct solar insolation, reflectance and scattering from adjacent surface regions may also influence the surface temperatures, especially in polar areas and in areas close to the terminator. Therefore it is necessary to include the local topography in equation 2, as it influences the insolation and temperatures as shown in figure 1.

Subsurface conduction, solar insolation and emission are part of the upper boundary condition (2). Shadowing of a surface may be caused by topography features in the direct line to the Sun. However, also insolation and emission angle may vary when observing a sloping surface. Surfaces with east-west facing slopes cause steeper gradients near sunrise and sunset. North-south facing slopes especially influence the insolation near local noon.

Due to topography, an observed surface emits radiation to other visible surface facets. However, this surface also receives scattered energy back from neighboring surfaces. This effect is similar to the reflectance of incident sunlight, which can be reflected from one surface to neighboring surfaces.

Results: Surface daytime temperatures are mainly controlled by their surface albedo and angle of incidence. However, nighttime temperatures are affected by changes in the thermal inertia. Topographic effects are expected to cause earlier or later sunrises and therefore high-standing areas receive sunlight for longer time, while sloping surfaces lead to a time displacement of the temperature cycle. For our model, some simplifications were necessary. As there are only

few landing sites on the Moon from which soil properties were determined, the subsurface conditions are considered as homogeneous over the whole planet. We assume a layered subsurface, similar to the model by [9], with a top layer of 2cm over a more dense and conductive bottom layer.

Lunar and Mercurian surface temperatures show the same general characteristics. Both have very steep temperature gradients at sunrise and sunset, due to the lack of an atmosphere (figure 2). Surface temperatures on the Moon vary about 280 K, on Mercury almost 600 K. However, there are major differences due to the orbital characteristics.

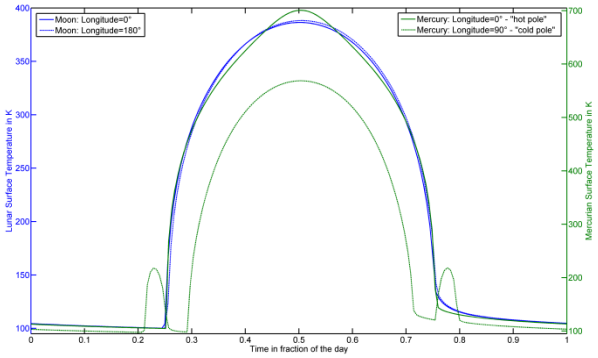

Figure 2: Comparison between flat-surface temperatures at different longitudes on the Moon (blue curve) and Mercury (green curve). The length of a lunar day is 29.5 Earth-days, a Mercurian day corresponds to 176 Earth-days.

At local noon, the near- and farside of the Moon receive sunlight under similar solar elevation angles. However, at this time of the lunar day the surface on the farside is slightly warmer than the nearside, because of the shorter distance to the Sun. During the orbit around the Sun the distance varies due to the eccentricity of the Earth-Moon-System, which results in different temperatures during a year.

On Mercury the 3:2 resonant rotation rate and the eccentric orbit cause distinct characteristics. At longitudes 0° and 180° local noon coincides with perihelion, which leads to a "warm pole". At longitudes 90° and 270° local noon coincides with aphelion, which results in a "cold pole". At these longitudes secondary sunrises and sunsets are visible, when Mercury's orbital angular velocity exceeds the spin rate during perihelion.

Conclusions: We developed a model that calculates surface temperatures on the Moon, which we extrapolated to Mercury. This model includes insolation cycles derived from JPL's Horizons software, brightness and topography of a study region, and scattering of solar insolation and infrared energy. Results obtained for the lunar surface show good agreement to Apollo, Clementine-LWIR and LRO-Diviner measurements. These results have shown, that the temperature- and depth-dependent thermophysical properties of the regolith can not be neglected, due to the large temperature variations over a lunar and Mercurian day.

The slow rotation and close distance to the Sun of Mercury requires a detailed analysis of shadowing effects at low elevation angles. During these times of the day, a fraction of the solar disk is below the horizon and the solar constant must be modified. The Sun can not be treated as a point source, as it would indicate darkness for areas where the sun is partially eclipsed. On the Moon this effect is less pronounced. Due to the larger distance the angular radius of the Sun is much smaller and the faster rotation period leads to relatively quick sunrises. However, when investigating polar areas, where the Sun is only partially visible over long times, or areas at local sunrise or sunset this effect needs to be included in the computation of solar insolation.

References: [1] Hiesinger, H. et al. (2010), *PSS 58*, 144-165. [2] Helbert, J. et al. (2005), *LPSC XXXVI*, Abstract #1753. [3] Keihm, S.J. and Langseth, M.G. (1973), *Proc. Lunar Sci. Conf. 4th*, 2503-2513. [4] Lawson, S.L. et al. (2000), *JGR 105*, E5, 4273-4290. [5] Pieters, C.M. et al. (2009), *Science 326*, 568-572. [6] Clark, R.N. (2009), *Science 326*, 562-564. [7] Sunshine, J.M. et al. (2009), *Science 326*, 565-568. [8] Bauch, K.E. et al. (2009), *LPSC XL*, Abstract #1789. [9] Vasavada, A. et al. (1999), *Icarus 141*, 2, 179-193. [10] Pike, R.J. (1988), *Mercury*, 165-273. [11] Ingersoll, A.P. et al. (1992), *Icarus 100*, 1, 40-47.

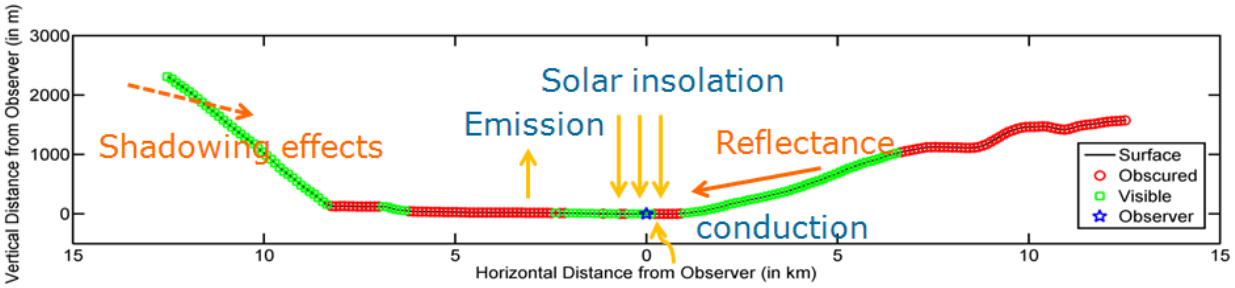

Figure 1: Topography profile showing effects on solar insolation due to local topography. Blue star marks observer's position, red circles denote areas that are shielded from the observer, green squares are visible areas.